GEOPHYSICAL TRANSACTIONS 1992
Vol. 37. No. 2-3. pp. 177-209

A PERCOLATION MODEL FOR THE PERMEABILITY OF KAOLINITE-BEARING SANDSTONES

Gábor KORVIN*

After a brief review of recent theories on the permeability of porous rocks, and of the rudiments of percolation theory, I shall develop a new model for the permeability of shaly sandstones containing discrete particle (kaolinite) clays. The experimentally found decrease in permeability for sufficiently high clay contents and low but non-zero porosities will be recognized as a percolation phenomenon, due to the blocking of a critical fraction of throats between the pore by kaolinite particles.

The main result is an expression for permeability (Eqs. 26a-f) in terms of grain size, porosity and kaolinite volume fraction. The expression contains a percolation factor $(p-p_c)^{PEX}$ which is identified with the divergence of the tortuosity near the percolation threshold. The percolation exponent *PEX* is simply connected to the fractal dimension of the tortuous fluid path.

The model was applied to compute the permeability of 229 kaolinite-bearing sandstone samples from Jurassic to Early Cretaceous fluvial and lacustrine reservoirs of the Eromanga Basin, South Australia. The coordination number of the approximating discrete percolation lattice and the percolation exponent were determined by computerised optimum search. There were no other adjustable parameters.

Fair agreement was found between the measured and computed permeabilities over more than 7 orders of magnitudes. Different percolation exponents were found for different lithologies: 0 for high permeability fine sand; 1.5-2 for coarse sand and siltstone; 3-5.5 for medium sand and 4.5-5.5 for low permeability (k < 100 md) fine sand.

Keywords: percolation, sandstone, permeability, fractals, models, kaolinite

* On leave from the Department of Geology and Geophysics, University of Adelaide, South Australia, Present address: PO Box 189, Rundle Mall, South Australia 5000

Manuscript received: 12 August, 1991

1. Historical introduction and problem discussion

1.1 Previous work on the permeability of shaly sandstones

The permeability of porous rocks can be expressed [WALSH, BRACE 1984] as:

$$k = \frac{1}{b} \Phi^3 \left(\frac{V}{A_s} \right)^2 \frac{1}{\tau^2} \tag{1}$$

where k is permeability, A_s /V is the surface area per unit volume, τ is tortuosity of the flow path and the constant b is equal to 2 for circular tubes and equal to 3 for cracks. An equivalent expression is:

$$k = \frac{R_{HYD}^2}{b} \Phi \frac{1}{\tau^2} \tag{2}$$

where R_{HYD} is the hydraulic radius, defined as the ratio of the pore volume to the wetted area. By definition [DULLIEN 1979], a porous material has a permeability of 1 darcy if a pressure difference of 1 atm produces a flow rate of 1 cm^3/sec of fluid with 1 cP viscosity through a cube having sides 1 cm in length. It is easy to check that 1 darcy = 0.987 μm^2, that is, if we express R_{HYD} in Eq. (2) in mm and k in millidarcies, the equation becomes:

$$k\,[md] = \frac{(R_{HYD}\,[mm])^2}{b} \Phi \frac{1}{\tau^2} 10^9 \tag{3}$$

The tortuosity in Eqs. (1-3) is between 2-4 in clean sands [VOLAROVICH et al. 1968], its role has generally been neglected in permeability studies. Equation (2) correctly describes the empirical fact [MARTIN, HAMILTON 1981] that permeability generally increases with increasing porosity. To find the grain-size dependence of permeability, assume spherical grains of radius r. Then a volume V of rock of porosity Φ will contain

$$N = V(1-\Phi) : \frac{4\,r^3\pi}{3} = \frac{3\,V(1-\Phi)}{4\,r^3\,\pi}$$

grains of total surface area:

$$A_s = N\,4\,r^2\,\pi = \frac{3\,V(1-\Phi)}{r}$$

That is, by Eq. (1) the permability can be expected to increase with the square of grain-size [MARTIN, HAMILTON 1981], or using a similar argument, with the square of the pore size [SERRA 1984].

It has recently been realized that the permeability of clay-bearing sandstones cannot be described by simple equations like (1) or (2) in a way universally valid for different values of clay content and for all clay morphologies. Any theoretical model attempting to describe fluid flow in shaly sands must conform with the following experimental facts:

a) The permeability of shaly sandstones rapidly decreases which increasing clay content and becomes almost zero (even for $\Phi > 0$) if the clay content is greater than about 15 % (HANIN [1951] cited in [EREMENKO 1968]. DENSON et al. [1968] also found that kaolinite clays in amounts of above 16 % reduce the permeability of sands with grainsize 0.3 mm ± 0.18 mm *SD* to practically zero.).

b) The relation between porosity and permeability depends on clay morphology. AMAEFULE et al. [1988] found different trends in the permeability versus porosity crossplots for reservoir sands, depending on whether the dominant clay minerals were of the 'pore bridging' (illite), 'pore lining' (chlorite) or 'discrete particle' (kaolonite) type [NEASHAM 1977].

c) The net confining pressure has a much larger effect on permeability than on porosity [AMAEFULE et al. 1988], the pressure sensitivity is strongly correlated with clay content [AMAEFULE et al. 1988] and is different for the various clay mineralogies [AMAEFULE et al. 1988].

As by Eq. (1) permeability is inversely proportional to the square of the internal surface-to-volume ratio of the rock, it is reasonable to assume that in shaly samples this ratio is affected, or even dominated, by the enormous specific surface of the clay particles [GOODE, SEN 1988, MICHAELS, LIN 1954]. (VAN OLPHEN, FRIPIAT [1979] quote 46 m^2/g specific surface for montmorrilonite, 8-13 m^2/g for kaolinite, 100 m^2/g for illite.) Since there is a well-established empirical correlation between the cation exchange capacity (*CEC*) and the specific surface of clays [PATCHETT 1975, STEWARD, BURCK 1986], GOODE, SEN [1988] have recently expressed the volume-to-surface ratio in Eq. (1) in terms of *CEC*. They deduced an expression:

$$k \approx C \Phi^m \frac{\Omega_+^2}{Q_V^2} \tag{4}$$

where C is an unknown constant, Q_V is charge per unit pore volume (computed from the measured values of *CEC* as:

$$CEC = \frac{Q_V \Phi}{[(1 - \Phi) \rho_g]} \tag{5}$$

ρ_g being grain density), Ω_+ is the surface charge density of clay, m is the (electric) tortuosity, determined by conductivity measurements [SEN et. al 1988].

Equation (4) is based on the assumption that the specific surface of the sand/clay composite is dominated by the surface areas of the clay particles. In Darcy's Law [DULLIEN 1979], however, we are only concerned with that part of the internal surface which actually becomes wetted. In case of pore lining (chlorite) or discrete particle (kaolinite) clays (using the classification of NEASHAM [1977]) only a small fraction of the total clay surface will be exposed to fluid flow and only in the case of pore bridging clays (illite) will most of the clay surface be wetted. Another problem with Eq. (4) is that it cannot explain the observed pressure sensitivity of the permeability of shaly sands. Because of the well-known experimental pressure dependence of porosity [HEDBERG 1926], the Goode-Sen model [GOODE, SEN 1988] (Eqs. 4 and 5) predicts a continuous decrease in permeability with increasing pressure and increasing clay content, rather than an abrupt disappearance of permeability at certain pressure and clay percentages.

To explain these discontinuous permeability changes we should have recourse to the Percolation Theory of Statistical Physics [DULLIEN 1979, ESSAM 1972, ZIMAN 1979, EFROS 1986].

1.2 Basic concepts of percolation theory

Historically, the very first published problem in percolation theory was a question related to the design of impermeable gas masks. It was raised by S. R. Broadbent — in abstract mathematical form — at a Symposium of the Royal Statistical Society on Monte Carlo Methods [BROADBENT 1954, HAMMERSLEY 1983]. At that time (1954) Broadbent was working at the British Coal Utilization Research Association on the design of gas masks for use in coal mines. The masks contained porous carbon granules into which the gas could penetrate. Broadbent found that if the pores were large enough and sufficiently well connected, the gas could permeate the interior of the granules; but if the pores were too small or inadequately connected, the gas would not get beyond the granules' surface. There was a critical porosity and pore interconnectedness, above which the mask worked well and below which it was ineffective. Thresholds of this sort are typical of percolation processes.

The basic result of percolation theory is represented in *Fig. 1* (after ZALLEN [1983]). In the (bond-) percolation problem we assume that a fraction $1-p$ ($0 \leq p \leq 1$) of the bonds of a regular grid are randomly cut and a fraction p are left uncut. Then there exists a critical fraction p_c (called percolation threshold) such that there is no continuous connection along

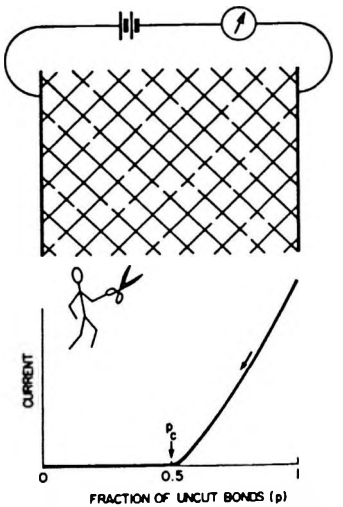

Fig. 1. Randomly cut network as example for percolation (after ZALLEN [1983])

1. ábra. Példa a perkolációra: négyzetrács véletlenszerűen elvágott élekkel. (ZALLEN [1983] nyomán)

Рис. 1. Пример перколяции: квадратная решетка со случайно пересеченный гранями (по ZALLEN [1983])

the bonds of the network between the opposite faces for $p < p_c$, and there exists a connection with probability 1 for $p > p_c$.

For the 2-dimensional square lattice (Fig. 1) the percolation threshold is 0.5. In the more general case the percolation threshold depends on the dimensionality of the network, d, and on its coordination number Z (where the coordination number is the average number of bonds connected to any node of the network), but it is independent of the detailed structure of the network. *Table I* (from ZIMAN [1979]) lists coordination numbers and

Network	Dimension d	Coordination number Z	p_c
Honeycomb	2	3	0.6527
Square	2	4	0.5
Triangular	2	6	0.3473
Tetrahedral (diamond)	2	4	0.39
Simple Cubic	3	6	0.25
Body Centered Cubic	3	8	0.18
Face Centered Cubic	3	12	0.12
Hexagonal Close Packing	3	12	0.12

Table I. Bond percolation tresholds
I. táblázat. Él-perkolációs küszöbértékek
Табл. I. Пороговые значения граневой перколяции

percolation thresholds for some common networks. It was first observed by VYSSOTSKY et al. [1961] that the percolation thresholds of Table I conform quite closely to the simple empirical rule:

$$Z p_c = \frac{d}{d-1} \tag{6}$$

For a 3-dimensional network $\frac{d}{d-1} = 1.5$, that is percolation only occurs if there are on the average more than 1.5 links to any node.

Close to the percolation threshold ($p > p_c$) the nodes which are connected with each other by continuous paths form large clusters of average size ξ called the correlation distance. The correlation distance diverges for $p \to p_c$ as:

$$\xi \sim (p - p_c)^{-\nu} \tag{7}$$

(see FISCH, HARRIS [1978]). For 3-dimensional networks we have [FISCH, HARRIS 1978]:

$$\nu = 0.83 \tag{8}$$

independently of the coordination number. Obviously, the percolation between two opposite nodes of a cluster, a distance ξ apart, takes place along tortuous zig-zag paths. Near the percolation threshold the length $L(\xi)$ of a typical zig-zag path will grow as a power of ξ:

$$L(\xi) \sim \xi^{\alpha} \quad \text{for} \quad p \to p_c,\ p > p_c \tag{9}$$

or using Eqs. (7 and 8):

$$L(\xi) \sim (p - p_c)^{-\beta} \quad \text{for} \quad p \to p_c,\ p > p_c \tag{10}$$

where, for 3-dimensional lattices $\beta = \nu\alpha = 0.83\ \alpha$. As the correlation length ξ is the natural length scale in percolation problems, we shall follow RITZENBERGER, COHEN [1984] and define the tortuosity τ of the percolation path as:

$$\tau = \frac{L(\xi)}{\xi} = \xi^{\alpha - 1} = (p - p_c)^{-0.83\,(\alpha - 1)} = (p - p_c)^{-\gamma} \tag{11}$$

The exponents describing the length and tortuosity of the paths are compiled in *Table II* for different percolation models.

Definition of the path	α in $L \sim \xi^{\alpha}$	β in $L \sim (p-p_c)^{-\beta}$	γ in $\tau \sim (p-p_c)^{-\gamma}$	Ref.*	Note
Correlation length ξ	1	0.83	0	a	3-D percolation
Minimum path	1.3	1.08	0.25	b,c	3-D percolation
Conductive path	1.35	1.12	0.29	d	3-D percolation-conduction
Self-avoiding random walk on uncut bonds	1.7	1.41	0.58	e	3-D percolation
Brownian motion in 3-D	2	1.66	0.83	f	
Brownian walk on a d_f-dimensional fractal	$\alpha=\frac{3}{2}d_f$	0.83	$0.83(\alpha-1)$	c	$\alpha=(3/2)d_f$ is called the 'Alexander-Orbach conjecture' [STANLEY 1986]
Brownian walk on a 3-D dimensional fractal	4.5	3.74	2.91		The pore space of certain sandstones forms an almost 3-dimensional fractal [WONG 1988]

Table II. Percolation exponents
(*REFERENCES: a— FISCH, HARRIS 1978; b—RITZENBERGER, COHEN 1984; c—STANLEY 1986; d—LUBENSKY 1977; e—LE GUILLOU, ZINN-JUSTIN 1977; f—MOSOLOV, DINARYEV 1987

II. táblázat. Perkolációs hatványkitevők
(*HIVATKOZÁS: a— FISCH, HARRIS 1978; b—RITZENBERGER, COHEN 1984; c—STANLEY 1986; d—LUBENSKY 1977; e—LE GUILLOU, ZINN; f—MOSOLOV, DINARYEV 1987

Табл. II. Перколяционные степени
(*ЛИТЕРАТУРА: a— FISCH, HARRIS 1978; b—RITZENBERGER, COHEN 1984; c—STANLEY 1986; d—LUBENSKY 1977; e—LE GUILLOU, ZINN; f—MOSOLOV, DINARYEV 1987

The exponent α in Eq. (9) has a simple physical meaning [RITZENBERGER, COHEN 1984]: for distances x smaller than ξ, α is the fractal dimension [MANDELBROOT 1982, KORVIN 1992] of the fluid paths between two nodes x apart.

1.3 Percolation models of rock permeability

The pore structure of a sedimentary rock can be converted to a discrete lattice model by letting the pores correspond to nodes and the throats to bonds. The coordination number of the pore system is defined as the average number of throats which connect each pore, it is a measure of connectivity of the network of pores [DULLIEN 1979, WARDLAW, MCKELLAR 1981] and can be determined experimentally by serial sectioning [DULLIEN 1979]. Recent theoretical work in continuum percolation [ELAM et al. 1984, HALPERIN et al. 1985] has proved the general applicability of discrete lattice models in simulating continuous problems, though the percolation transport exponents for conductivity and permeability have been found larger than their discrete lattice counterparts [HALPERIN et al. 1985].

Early application of percolation theory centred around qualitative problems of oil recovery [DULLIEN 1979] and mercury porosimetry [WARDLAW, MCKELLAR 1981]. Recent, quantitative results are reviewed by THOMPSON et al. [1987] and WONG [1988]. In 1985 HALPERIN et al. [1985] at the Harvard University introduced a 'Swiss cheese' permeability model in which the holes play the role of sand grains and the cheese is the flowing water. They found that if we make more and more holes there is a critical fraction of cheese $\Phi_c \approx 0.03$–0.04 at which electric conductivity vanishes as $(\Phi - \Phi_c)^t$ and hydraulic permeability vanishes as $(\Phi - \Phi_c)^e$, with t=2.4 and e=4.4. In an important paper KATZ, THOMPSON [1986] of Exxon Production Research, Houston, assumed that only throats wider than a given characteristic length l_c can significantly contribute to permeability and then applied percolation arguments to derive permeability in the form:

$$k = \beta \Phi l_{\max}^2 [p(l_{\max}) - p(l_c)]^t \tag{12}$$

with $\beta = 1/32$; for t they simply took the percolation conductivity exponent [FISCH, HARRIS 1978] t=1.9. In Eq. (12) $p(l)$ means the probability that a throat is wider than l; l_c is a critical width such that the throats wider than l_c still form a connected net across the rock; l_{max} is another size parameter. The critical width l_c can be experimentally determined using mercury intrusion [KATZ, THOMPSON 1986].

In the present study I shall develop a percolation-theoretical model for the permeability of kaolinite-bearing sandstones from oil reservoirs of the Eromanga Basin, South Australia. I shall prove that there is a percolation threshold at some critical kaolinite content, and that the tortuosity of the flow path (figuring in Eq. 2) diverges at the percolation threshold as described in Eq. (11).

The main result is contained in Eqs. (26a–f), which is formally similar to the KATZ, THOMPSON [1986] equation (12), but the power-like disap-

pearance of permeability at the percolation threshold is attributed here to the divergence of tortuosity.

The results are only applicable to 'discrete particle' [NEASHAM 1977] clay morphologies (as kaolinite). Possible extensions to pore lining and pore bridging [NEASHAM 1977] clays will be mentioned at the end of the paper.

2. Materials and methods

2.1 Previous studies of eromanga basin petrophysics [GRAVESTOCK, ALEXANDER 1986, 1988, 1989]

The Eromanga Basin, Australia's largest onshore hydrocarbon province, covers an area approximately 1,000,000 sq km, within which up to 3,000 m of Jurassic to Late Cretaceous sediments are preserved. The sequence consists of a lower suite of continental deposits which unconformably overlie deeper Palaeozoic basins or older metamorphic and igneous rocks, and an upper suite of transgressive marine sediments which in turn are overlain by thick paralic to continental strata. Numerous oil and gas accumulations have been discovered in the lower suite over the past 10 years.

In 1985, the South Australian Department of Mines and Energy commenced a study of the petrophysics of Eromanga Basin reservoirs. Funding for the project was provided by the Commonwealth Department of Primary Industries and Energy (NERRDDC Project 820). Cores from 18 wells were selected for analysis (*Fig. 2, Table III*) and 638 cylindrical

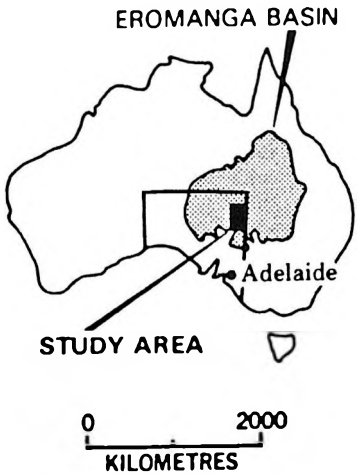

Fig. 2. Location map of the study area
2. ábra. A kutatási terület sematikus térképe
Рис.2. Карта-схема участка

core plugs were cut from lithologies ranging from coarse sandstones to mudrocks. Petrophysical analyses were carried out by the Australian Mineral Development Laboratories (AMDEL Ltd., Adelaide, South Australia).

Mid-core depth (m)	Number of samples			
	Porosity and permeability	Grain density and *CEC*	XRD	Electrical properties
1207.5	31	9	4	4
1209.8	26	14	-	-
1243.0	7	3	1	2
1247.7	29	11	4	4
1434.6	65	28	4	7
1448.4	26	10	-	5
1495.5	14	8	-	-
1505.2	42	14	4	-
1564.2	16	8	3	2
1571.2	22	11	-	3
1587.2	21	10	-	2
1608.1	35	12	4	4
1635.2	16	7	1	-
1682.7	35	10	4	-
1693.9	92	37	6	12
1797.7	49	10	5	-
1843.9	61	20	3	9
1878.5	22	9	-	4
2166.2	7	3	-	-
2663.1	22	12	4	2
Total	638	246	47	60

Table III. Summary of petrophysical measurements
The results are tabulated in GRAVESTOCK, ALEXANDER [1988]

III. táblázat. A kőzetfizikai mérések összesitése
GRAVESTOCK, ALEXANDER [1988]

Табл. III. Обзор измерений физических свойств
GRAVESTOCK, ALEXANDER [1988]

All plugs were cut, trimmed, and measured for effective porosity by helium injection and horizontal permeablility to nitrogen (not Klinkenberg corrected) at overburden pressure.

Absolute grain density and cation exchange capacity (*CEC*) were determined on 246 plugs. Forty-seven samples were subject to X-ray diffraction analysis to find the distribution of the bulk mineralogy and the mineralogy of the < 2 μm fraction. Sixty samples were submitted for electrical properties determination, using simulated formation brines, twenty-one of these had repeat measurements of conductivity in NaCl brines of differing salinity. Results are tabulated in GRAVESTOCK, ALEXANDER [1988]. Five grain size categories were selected by visual examination: coarse-, medium- and fine sandstone, siltstone and mudrock. Fine sandstone samples were further sub-divided into two sets: those with permeability of 100 md or more, and those with less than 100 md permeability.

2. 2 *Petrophysical properties*

The petrophysical properties relevant to this paper are summarised in Figs. 3–8.

Figure 3 shows the porosity distribution for the selected visual grain size categories. In spite of the considerable overlap between the porosity ranges there is a clear decreasing trend in average porosity with decreasing grain size. A similar trend has been observed for the Permian reservoir rocks of the Cooper Basin, underlying the Eromanga Basin [MARTIN, HAMILTON 1981, SCHULZ-ROJAHN, PHILLIPS 1989]. When unconsolidated marine sediments are considered the grainsize—porosity relation is just the opposite (that is, the smaller the grain size the higher the porosity [HAMILTON 1972]), we assume that the trend shown by Figure 3 is due to the differences in compaction and diagenesis acting on sediments of different grain size.

The permeability vs. porosity cross plots (*Fig. 4*) show completely different patterns in the different visual grain-size ranges. The cross plot for 'fine sands' (shown twice in Fig. 4) reveals a dual character corresponding to the high permeability (k >100 md) and low permeability (k <100 md) categories. GRAVESTOCK, ALEXANDER [1986] emphasised that two porosity-permeability trends were apparent. They later [GRAVESTOCK, ALEXANDER 1988] provided empirical equations for each trend.

Semi-quantitative X-ray diffraction data for 47 samples are summarised in *Fig. 5*, which shows the distribution of the bulk mineralogy and of the < 2 μm fraction as function of the visual grain size of the host facies for each sample. The bulk mineralogy is quartz dominated whereas the clay size fraction is chiefly kaolinite, other minerals being relatively minor. The < 2 μm fraction rarely exceeded 20 percent by weight of the bulk sample.

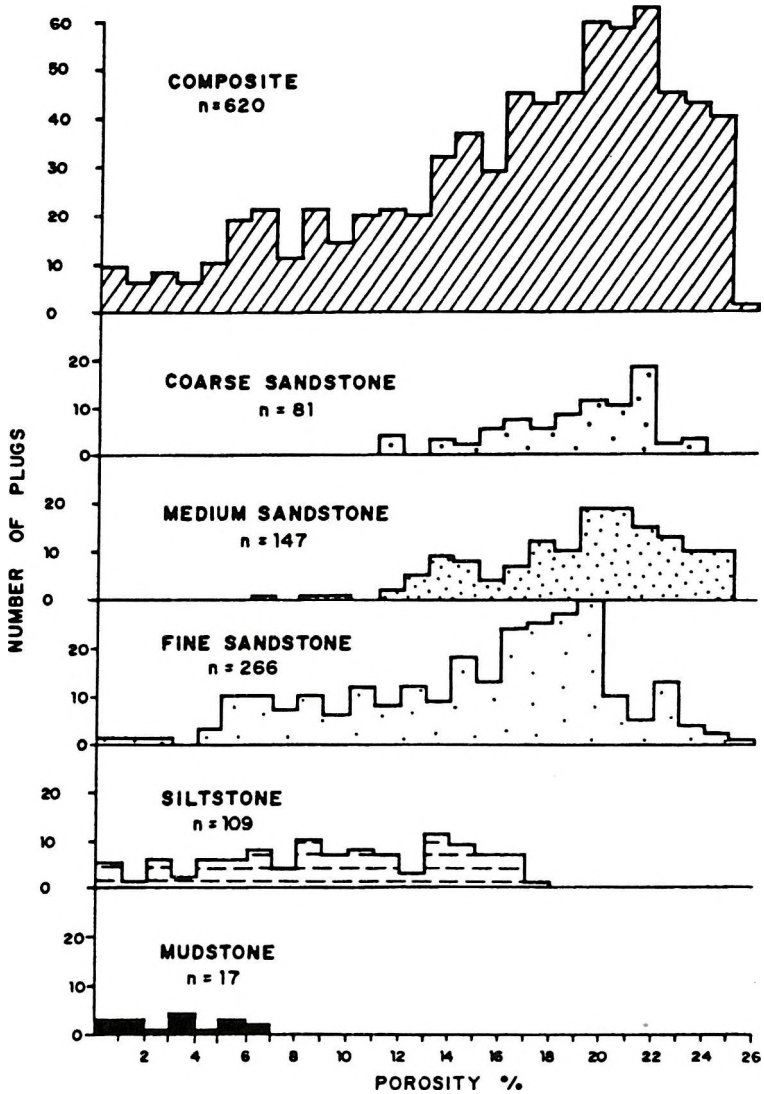

Fig. 3. Porosity distribution by visual grain-size [from GRAVESTOCK, ALEXANDER 1988]

3. ábra. A porozitás eloszlása különböző szemcseméretek esetében [GRAVESTOCK, ALEXANDER 1988]

Рис.3. Распределение пористости при различных размерах зерен [GRAVESTOCK, ALEXANDER 1988]

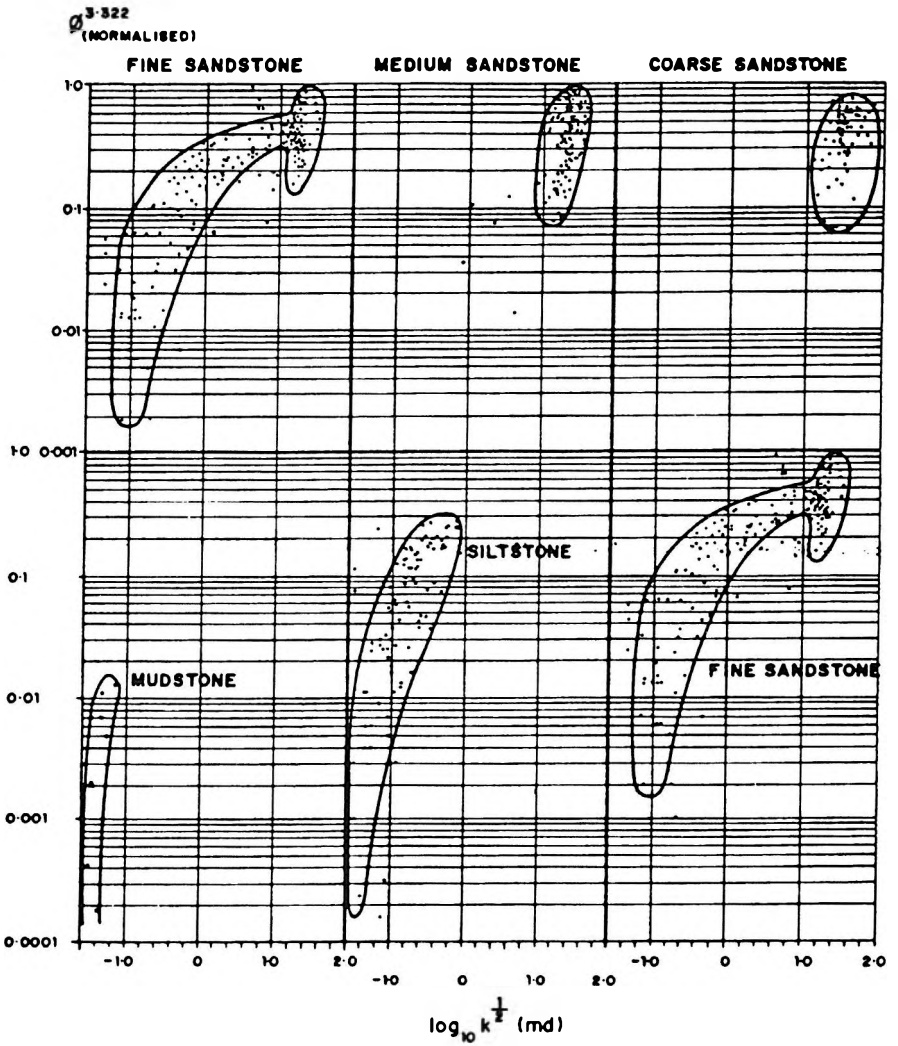

Fig. 4. Porosity—permeability trends by visual grain-size [from GRAVESTOCK, ALEXANDER 1988]

4. ábra. Porozitás—permeabilitás trendek különböző szemcseméretek esetében [GRAVESTOCK, ALEXANDER 1988]

Рис. 4. Тренды пористости—проницаемости при различных размерах зерен [GRAVESTOCK, ALEXANDER, 1988]

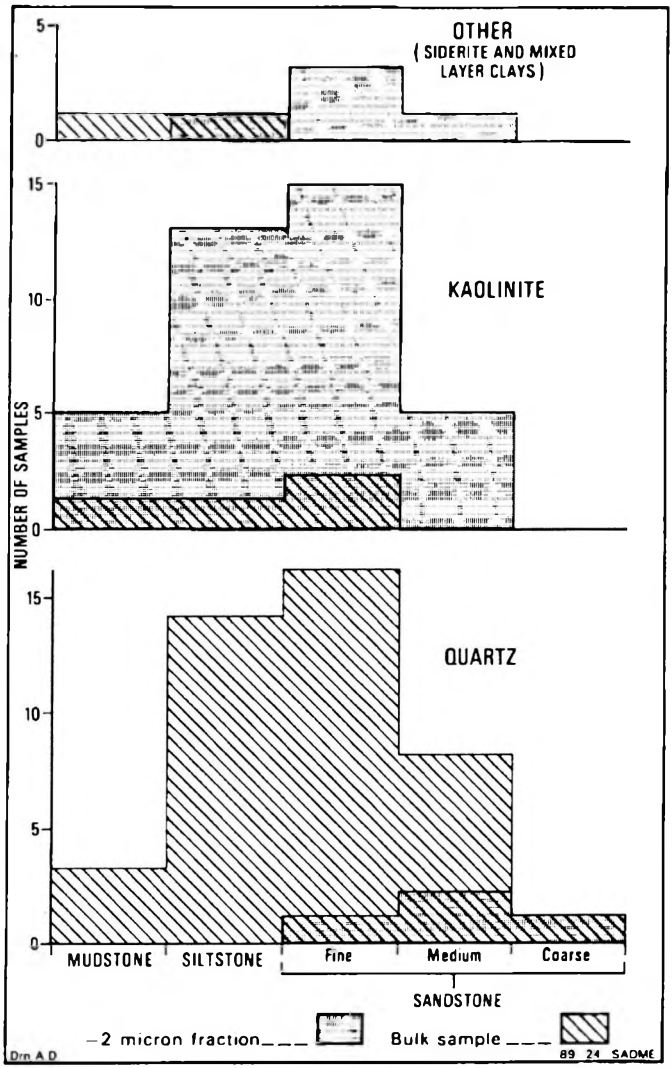

Fig. 5. Distribution of bulk and < 2 μm mineralogy determined by semi-quantitative X-ray diffraction, as a function of visual grain-size of the host facies [from GRAVESTOCK, ALEXANDER 1988]

5. ábra. A teljes minta, ill. a < 2 μm frakció, fél-kvantitatív röntgen-diffrakcióval meghatározott ásványtartalom eloszlása, különböző szemcseméretű hordozókőzetek esetében [GRAVESTOCK, ALEXANDER 1988]

Рис.5. Распределение минерального состава полной пробы и фракции меньше 2 мкм, определенного полуколичественным рентген-дифракционным способом для вмещающей породы с различным размером зерен [GRAVESTOCK, ALEXANDER 1988]

Clay minerals of relatively low electrical activity were indicated from *CEC* measurements of 246 samples whose values range from less than 1.0 to 10 meq /100 g, which is the typical range of kaolinite (*Table IV*).

Name	*CEC* meq/100 g	Ref.*
Kaolinites	3-15 4.9 (mean) 3-25	a b c
Illites	10-40 26.6 (mean) 20-30	a, c b d
Chlorite	10-40	a, c
Smectite	80-150	a, c
Montmorillonite	100-250 82.5	d b

Table IV. Cation exchange capacity of clay minerals
(*REFERENCES: a—GRIM 1968; b—VAN OLPHEN, FRIPIAT 1979; c—EDMUNDSON, RAYMER 1979; d—PATCHETT 1975)
IV. táblázat. Agyagásványok kation csere kapacitása
(*HIVATKOZÁS: a—GRIM 1968; b—VAN OLPHEN, FRIPIAT 1979; c—EDMUNDSON, RAYMER 1979; d—PATCHETT 1975)
Табл. IV. Емкость обмена катионов глинистых минералов
(*ЛИТЕРАТУРА: a—GRIM 1968; b—VAN OLPHEN, FRIPIAT 1979; c—EDMUNDSON, RAYMER 1979; d—PATCHETT 1975)

According to literature, there is a good overall correlation between *CEC* and the specific surface of clays [PATCHETT 1975 , STEWARD and BURCK 1986]. In the present case the dominant clay mineral is presumed to be kaolinite which has a distinct narrow range of *CEC* values (Table IV). *Figure 6* shows the correlation between *CEC* and weight percent of the < 2 μm fraction for 27 samples. The relationship can be approximated by the empirical equation

$$\lambda = 0.021\ CEC \tag{13}$$

where *CEC* is in meq /100 g, λ is the weight proportion of the clay size (< 2 μm) fraction, determined from semiquantitative XRD [GRAVESTOCK, ALEXANDER 1988]. I shall assume that in the Eromanga Basin samples the greatest part of the clay size fraction actually consists of clay minerals (as found in other parts of the world [KUKAL, HILL 1986]) and that it is predominantly kaolinite as indicated by the *CEC* and XRD data. Also, as there is only a slight difference between the densities of quartz

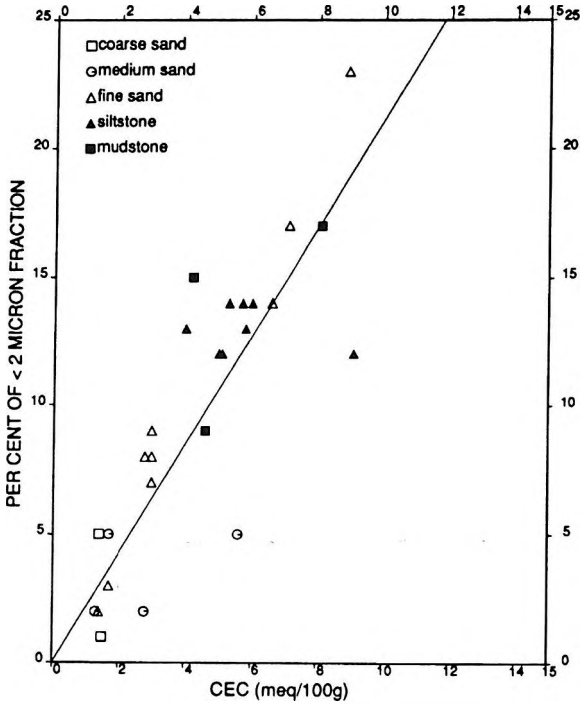

Fig. 6. Correlation between cation exchange capacity (*CEC*) and weight percent (λ) of the < 2 μm fraction. Equation of the straight line is λ = 0.021 *CEC*. The λ values were determined [by GRAVESTOCK, ALEXANDER 1988] from semiquantitative XRD

6. ábra. Korreláció a kation csere kapacitás (*CEC*) és a < 2 μm frakció súlyaránya (λ) között. A regressziós egyenes egyenlete λ = 0.021 *CEC*. A λ értékek meghatározás [GRAVESTOCK, ALEXANDER 1988] fél-kvantitatív röntgendiffrakción alapult

Рис. 6. Корреляция между емкостью обмена катионов (*CEC*) и весового содержания (λ) фракции меньше 2 мкм. Уравнение линии регрессии λ = 0.021 *CEC*. Определение величины λ основано на данных полуколичиественного рентген-дифракционного способа [GRAVESTOCK, ALEXANDER 1988]

[SERRA 1984] and kaolinite [GRIM 1968], I shall identify the λ in Eq. (13) with the volume fraction of kaolinite.

Previous studies of GRAVESTOCK, ALEXANDER [1988] have already indicated that *CEC* values can be used to judge reservoir quality: good reservoir sandstones (k >100 md) have *CEC* values less than 3.0 meq/100 g whereas fine grained, shaly sediments with fair to nil reservoir quality have higher *CEC*'s (*Fig. 7*). The main task of the next section will be to develop this empirical observation into a physical theory of the permeability of kaolinite bearing sandstones.

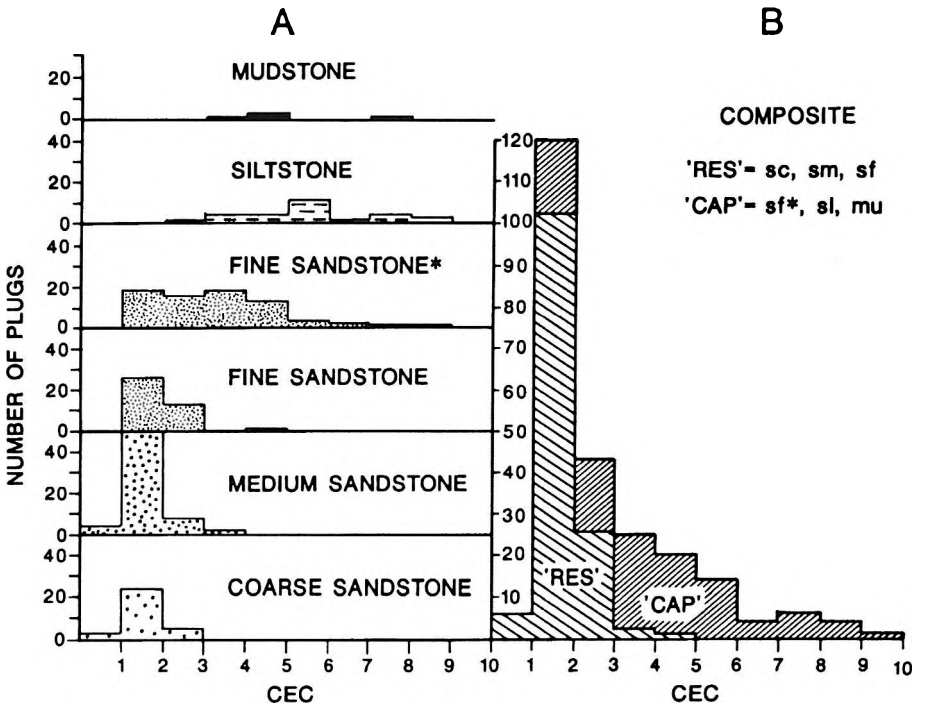

Fig. 7. Cation exchange capacity distribution with visual grain-size (A); and CAP and RES trend distribution with *CEC* (B) (CAP=caprock, RES=reservoir, sc=clean sand, sm=medium sand, sf=clean fine sand, sf*=shaly fine sand, si=siltstone, mu=mudstone) [from GRAVESTOCK, ALEXANDER 1988]

7. ábra. Kation csere kapacitás (*CEC*) eloszlása különböző szemcseméretekre (A); és a fedőkőzet ill. tárolókőzet trendek eloszlása különböző *CEC* értékekre (B). (CAP=fedőkőzet, RES=tárolókőzet, sc=tiszta homokkő, sm=közepes szemcseméretű homokkő, sf=finomszemcsés tiszta homokkő, sf*=agyagos finomszemcsés homokkő, si=homokliszt, mu=agyagpala). [GRAVESTOCK, ALEXANDER 1988]

Рис. 7. Распределение емкости обмена катионов (*CEC*) для разных размеров зерен (A) и распределение трендов покрывающих и вмещающих образований при разных значениях *CEC* (B). (CAP =покрывающие образования, RES=вмещающие породы, sc=чистые песчаники, sm=среднезернистые песчаники, sf=мелкозернистые чистые песчаники, sf*=глинистые мелкозернистые песчаники, si=печаные илы, mu=глинистые сланцы). [GRAVESTOCK, ALEXANDER 1988]

3. The percolation model

3.1 Theoretical derivation

In order to describe the permeability of the Eromanga Basin reservoir sandstones I start out from the formula [WALSH, BRACE 1984]:

$$k\,[md] = \frac{(R_{HYD}\,[mm])^2}{b}\,\Phi\,\frac{1}{\tau^2}\,10^9 \tag{3}$$

and express the hydraulic radius R_{HYD} and tortuosity τ in terms of grain radius (r), porosity (Φ) and kaolinite content (λ).

As we assume cylindrical tubes, b is taken as 2 [WALSH, BRACE 1984]. In a simplified rock model where the < 2 μm fraction consists of kaolinite, a volume V_0 of the rock will consist of:

$$V_1 = V_0\,(1 - \Phi)\,(1 - \lambda) \quad \text{quartz} \tag{14a}$$

$$V_2 = V_0\,(1 - \Phi)\,\lambda \quad \text{kaolinite} \tag{14b}$$

$$V_3 = V_0\,\Phi \quad \text{pore} \tag{14c}$$

It is assumed that the volume fraction λ of kaolinite can be expressed in terms of *CEC* by the empirical equation (13). If the average radius of a quartz grain is r, the total quartz volume V_1 contains

$N = \dfrac{V_0\,(1 - \Phi)\,(1 - \lambda)}{4/3\,r^3\,\pi}$ grains, that is in a volume V_0 of rock the total surface of quartz grains is:

$$S_{tot,\,quartz} = N\,4\,r^2\,\pi = \frac{3\,V_0\,(1 - \Phi)\,(1 - \lambda)}{r} \tag{15}$$

If (in thought) we remove all clay particles, an increased space $V_2 + V_3 = V_0\,[(1 - \Phi)\,\lambda + \Phi]$ will be available for fluid flow.

As a cylinder of length h and radius R has a volume $V = R^2\pi h$ and surface area (without the bases) $S = 2\,R\pi h$, that is $R = (2\,V)/S$; we find from Eqs. (14 and 15) that the space $V_2 + V_3$ can be considered as a very long cylinder of average radius:

$$r_2 = \frac{2\,(V_2 + V_3)}{S_{tot,\,quartz}} = \frac{2}{3}\,\frac{\Phi + (1 - \Phi)\,\lambda}{(1 - \Phi)\,(1 - \lambda)}\,r \tag{16}$$

If we put back again the kaolinite particles the radius of the cylinder will be reduced to r_1, $r_1 < r_2$ because kaolinite sticks to the walls. As all the pore space is contained within the long cylinder of radius r, and all the clay particles are dispersed within the ring $r_1 \leq r \leq r_2$ we can write:

$$\frac{r_1^2}{r_2^2} = \frac{\Phi V}{[\Phi V + (1 - \Phi)\lambda V]}$$

that is

$$r_1 = r_2 \sqrt{\frac{\Phi}{\Phi + (1 - \Phi)\lambda}} = r_2 \sqrt{p} \tag{17}$$

where we have introduced the notation

$$p = \frac{\Phi}{[\Phi + (1 - \Phi)\lambda]} = \frac{V_3}{(V_2 + V_3)} \tag{18a}$$

Obviously, $0 \leq p \leq 1$; p has a simple physical meaning: it is the ratio of open pore space to the total space filled by pores or clays. We shall also need the proportion of clay in this space, it is

$$q = 1 - p = \frac{\lambda(1 - \Phi)}{[\Phi + (1 - \Phi)\lambda]} = \frac{V_2}{(V_2 + V_3)} \tag{18b}$$

As in Darcy's Law [DULLIEN 1979] the hydraulic radius R_{HYD} is defined as the flow cross sectional area divided by the wetted perimeter, in Eq. (3) we shall use

$$R_{HYD} = \frac{r_1^2 \pi}{2 r_1 \pi} = \frac{r_1}{2} \tag{19}$$

If we assume a constant tortuosity and substitute Eqs. (16-19) into Eq. (2) we find that for any given kaolinite volume fraction λ the permeability would tend to zero as a power of Φ and that it is impossible to have zero permeability for finite (non zero) porosities. To be able to explain the experimental data (*viz.* the very low or zero permeabilities above a certain clay content, see Fig. 7) I shall transform the continuous Darcy flow to a lattice percolation problem. Let us make the pores of the rock correspond to the nodes of a discrete lattice, throats will correspond to the bonds (*Fig. 8*, where the symbolic 'current' represents hydraulic flow). If a given throat is completely blocked by kaolinite the corresponding bond will be considered as 'cut' otherwise it is 'uncut', independently of the actual radius of

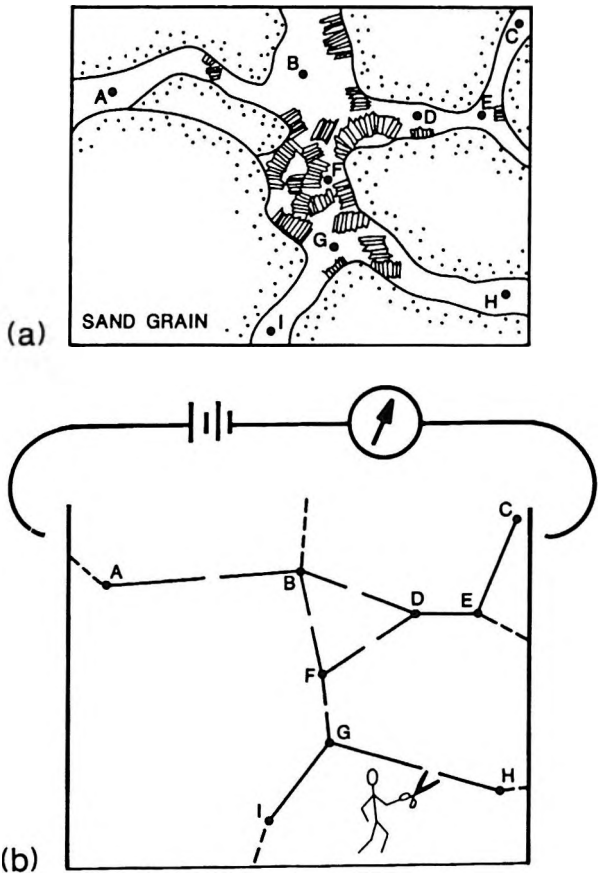

Fig. 8. Fluid transfer through kaolinite-bearing sandstone (a) and the corresponding lattice percolation model (b). Nodes correspond to pores, uncut bonds to open throats, cut bonds to throats blocked by kaolinite particles. The symbolic 'current' can be an arbitrary transfer process

8. ábra. Folyadék-áramlás kaolinit-tartalmú homokkövön keresztül (a), és a megfelelő diszkrét perkolációs model (b). A pórusoknak csomópont, nyílt toroknak elvágatlan él, a kaolinit részecskék által eltorlaszolt toroknak elvágott él felel meg. A szimbolikus "áram" tetszőleges átviteli folyamat lehet

Рис.8. Миграция жидкости через каолинит-содержаший песчаник (а) и отвечающая ей дискретная перколяционная модель (b). Порам соответствует точка, открытым горловинам - непересеченная грань, а закрытым горловинам- пересеченная грань. Символическому току может отвечать любой процесс переноса

the throat. The coordination number Z of the network depends on the original packing of the quartz grains and on subsequent compaction and diagenesis history. As the number of long-, concavo-convex and sutured

contacts between grains increases with depth and age of the rock [TAYLOR 1950, SMALLEY 1967], the coordination number Z will generally decrease with increasing compaction (note the missing bond in Fig. 8b between nodes A and F, because of the concavo-convex contact between the adjacent grains). Generally, Z ranges between 1 and 6 for sandstones. Using the empirical rule [VYSSOTSKY et al. 1961]:

$$Z\,p_c = \frac{d}{(d-1)} \tag{6}$$

and assuming a 3-dimensional lattice, the bond percolation threshold probability becomes

$$p_c = \frac{1.5}{Z} \tag{20}$$

Because kaolinite is distributed as discrete book-like clusters (Fig. 8a), I assume that any given throat connecting adjacent pores is open with probability p and blocked by kaolinite particles with probability q (Eqs. 18a,b). In the equivalent lattice percolation problem (Fig. 8b) a fraction q of the bonds are randomly cut, and a fraction $p = 1 - q$ are left intact.

By the definition of the percolation threshold, the fluid cannot flow through the sample for $p < p_c$ and percolation only starts for $p > p_c$. Generally, the fluid particles will follow complicated zig-zag paths, the closer is p to p_c, the greater will be the length $L(x)$ of a typical flow path between two nodes, which are in a geometrical sense only a distance x apart.

As it was shown in Section 1.2, for $p \to p_c$ the tortuosity tends to infinity as

$$\tau \sim (p - p_c)^{-0.83\,[\alpha - 1]} \tag{11}$$

that is $\frac{1}{\tau^2}$ of the permeability equation (2) or (3) will tend to zero as

$$\frac{1}{\tau^2} \sim (p - p_c)^{1.66\,[\alpha - 1]} \tag{21}$$

In Eqs. (11 and 21) α ($\alpha \geq 1$) is the fractal dimension [RITZENBERGER and COHEN 1984] of the percolation path for small distances. Let us define a percolation function *PERC* as

$$PERC\,(p) = \begin{cases} 0 & \text{if } p \leq p_c \\ C_0\,(p - p_c)^{1.66\,[\alpha - 1]} = C_0\,(p - p_c)^{PEX} & \text{if } p \geq p_c \end{cases} \tag{22}$$

where *PEX* (percolation exponent) is defined as

$$PEX = 1.66\,(\alpha - 1) \tag{23}$$

and the normalizing constant C_0 is chosen as to make $PERC(1)=1$, that is

$$C_0 = \frac{1}{(1 - p_c)^{PEX}} \tag{24}$$

We still have to find the constant factor τ_0 in the tortuosity function

$$\frac{1}{\tau^2} = \frac{1}{\tau_0^2}\, PERC(p) \tag{25}$$

For clean sandstones $\lambda = 0$, consequently $p=1$ and $PERC(1)=1$, that is for τ_0 we must choose some average tortuosity value which is characteristic to clean sands in the ambient pressure range of the Eromanga Basin reservoir rocks [GRAVESTOCK and ALEXANDER 1988] (12,500–22,000 kPa). According to high-pressure studies [VOLAROVITCH et al. 1968] $\tau_0 = 4$ seems a reasonable choice.

Combining Eqs. (3, 13 and 16-25) the final expression for k becomes

$$k = \begin{cases} \dfrac{R_{HYD}^2}{b\,\tau_0^2}\,\Phi\,10^9\,\dfrac{(p - p_c)^{PEX}}{(1 - p_c)^{PEX}} & \text{if } p \geq p_c \\ 0 & \text{if } p \leq p_c \end{cases} \tag{26a}$$

with

$$b = 2, \quad \tau_0 = 4 \tag{26b}$$

$$R_{HYD} = \frac{1}{3}\,\frac{\Phi + (1 - \Phi)\,\lambda}{(1 - \Phi)\,(1 - \lambda)}\, r\sqrt{p} \tag{26c}$$

$$\lambda = 0.021\,CEC \tag{26d}$$

$$p = \frac{\Phi}{[\Phi + (1 - \Phi)\,\lambda]} \tag{26e}$$

$$p_c = \frac{1.5}{Z} \tag{26f}$$

Equation (26) is the main result of the present paper. In the actual application of these expressions to Eromanga Basin sandstones, the coordination number Z and the percolation exponent PEX were determined numerically. I assumed various Z and PEX values ($1 \leq Z \leq 6$; $1 \leq PEX \leq 6$), computed the permeabilities $k_{comp}(Z,PEX)$ for all samples and then minimised the error

$$DEV(Z, PEX) = \sum [\log k_{meas} - \log k_{comp}(Z, PEX)]^2 \qquad (27)$$

with respect to Z and PEX.

Note that Eq. (26) has the same form as the Katz-Thompson [1986] percolation equation

$$k = \beta \Phi l_{max}^2 [p(l_{max}) - p_c)]^t \qquad (12)$$

even the constant factors are the same ($\beta = \frac{1}{32}$ in Eq. (12) and $\frac{1}{(b \tau_0^2)} = \frac{1}{32}$ in Eq. (26)).

Equation (26) of the present paper, however (which strictly speaking only applies to kaolinite-bearing sands) has been derived using quite different arguments, and the percolation factor $(p - p_c)^{PEX}$ corresponds to the normalized reciprocal squared tortuosity of the fluid paths near the percolation threshold.

3.2 Application to the Eromanga Basin reservoir rocks

I applied the percolation model of Eqs. (26a-f) to compute the permeabilities of 229 sandstone samples from Eromanga Basin reservoirs. In the computations I used measured values of porosity and of cation exchange capacity (CEC), and visual grain size estimations. I assumed that the clay size (< 2 μm) fraction behaves as kaolinite for all samples, in the sense that the permeability reduction is due to the blocking of a part of the throats by discrete clusters of clay particles. The clay volume content was estimated from the measured CEC using Eq. (13). The percolation parameters Z and PEX had been numerically optimised for each lithology class. The main problem in applying Eqs. (26) to the real data has been that in Eq. (26c) we need a numerical value for the mean grain radius r. First, I identified the qualitative lithologic classes with the Wentworth size classes [PETTIJOHN et al. 1972] (see Table V) and defined $\bar{r}$ as the radius of a particle at the middle of the corresponding size range, that is $\bar{r}$ = 0.375; 0.1875; 0.094; 0.094; 0.02 for the respective lithologies 1, 2, 3, 4 and 5 (Table V). As this

Lithology Number	Code	Name	Wentworth Size Range (mm)	$\bar{r}$	No. of samples	Φ_{min}	Φ_{max}	Z_{opt}	PEX_{opt}
1	❑	Coarse sandstone	1-0.5	0.375	31	0.11	0.24	2.5	1.5
2	○	Medium sandstone	0.5-0.25	0.188	57	0.06	0.25	2.5	3.0
3	■	High k (clean) fine sandstone	0.25-0.125	0.094	37	0.0	0.26	-	0
4	Δ	Low k (shaly) fine sandstone	0.25-0.125	0.094	74	0.0	0.26	6.0	5.5
5	▲	Silstone	0.0625-0.0039	0.02	30	0.0	0.18	6.0	2.0

Table V. Summary of data used to construct Figure 9
V. táblázat. A 9. ábra szerkesztéséhez felhasznált adatok
Табл. V. Данные, использованные при составлении рис.9.

resulted in an unreasonable large scatter in k_{comp}, I decided to estimate graintsize within the allowed range by assuming some smooth dependence on porosity. After many trials and errors I have found that the best way for approximating the grain size of any sample of a given lithology i (i=1, 2,..., 5) is to linearly interpolate the logarithm of the grain size between the Wentworth limits as Φ varies between the measured bounds $\Phi^{(i)}_{min}$ and $\Phi^{(i)}_{max}$:

$$\log 2r(i) = \log 2r_{max}(i) + \frac{\Phi - \Phi_{min}(i)}{\Phi_{max}(i) - \Phi_{min}(i)} [log 2r_{max}(i) - \log 2r_{min}(i)]$$

$$(i = 1, 2, ...,5) \qquad (28)$$

(The grainsize-porosity dependence of Eq. (28) is in accord with the results of HAMILTON [1972] for recent marine sediments.)

The optimal coordination number Z_{opt} and percolation exponent PEX_{opt} were separately determined for each lithology. I computed k from Eqs. (26a-f) and Eq. (28) for different values of Z and PEX ($2 \le Z \le 6$; $1 \le PEX \le 6$) and determined Z_{opt} and PEX_{opt} as to minimise the error between the logarithms of the measured and computed permeabilities. Using the optimised values of Z and PEX (compiled in Table V) a fair agreement was obtained between measured and computed permeabilities over seven orders of magnitude (*Fig. 9*). The optimisation of expression

(27) with respect to Z and PEX was not unambiguous: as shown in *Fig. 10* for each lithology there are distinct clusters of suboptimal parameters (Z, PEX) around the optimal (Z_{opt}, PEX_{opt}) which were found almost as effective in optimising the error, apart from insignificant digits.

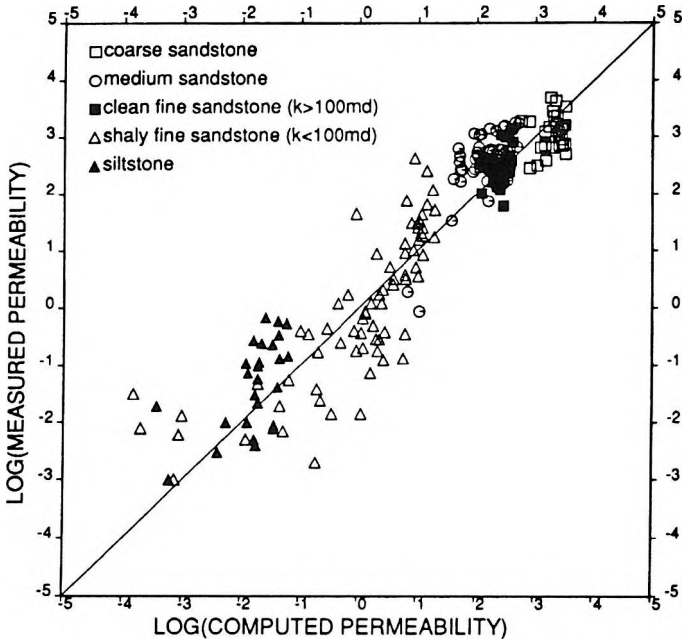

Fig. 9. Crossplot of measured vs. computed permeabilites

9. ábra. Mért permeabilitás — számított permeabilitás crossplot

Рис. 9. Связь между измеренной и вычисленной проницаемостью

4. Discussion and conclusions

Using the optimised percolation parameters (Table V) I could keep the deviation between measured and computed permeabilities within order of magnitude limits, except for a few fine-grained samples (Fig. 9). The scatter is due to three factors:

a) visual, rather than quantitative, average grain-size estimation; samples frequently displayed a range of grain sizes of several phi units;

b) difficulties in measuring very low permeabilities; and

c) using an insufficient number of semiquantitative XRD data to express kaolinite volume content in terms of *CEC* (Eq. 13).

As by Eqs. (26a,c) permeability is proportional to the squared radius of quartz grains, if grain size is only known qualitatively to belong to a given Wentworth scale class this involves a scatter of $\pm\log_{10}2^2 = \pm 0.6$ in $\log k_{comp}$.

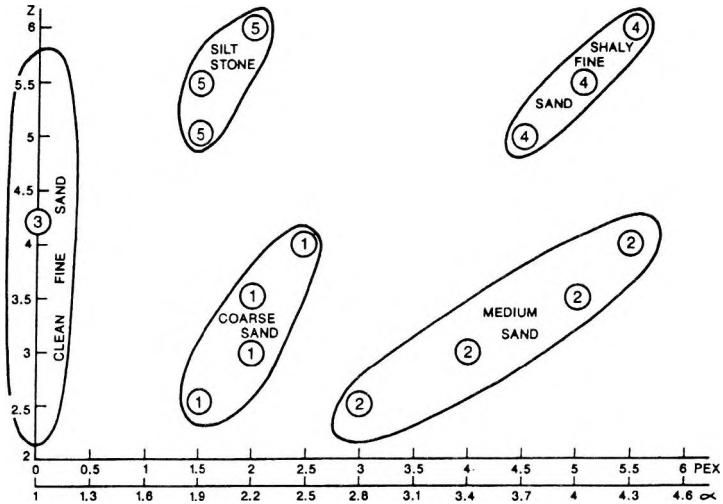

Fig. 10. Optimal percolation parameters *Z* and *PEX* for the different lithologies (*Z*=coordination number, *PEX*=percolation exponent, α =fractal dimension of the tortuous flow path)

10. ábra. Optimális perkolációs paraméterek különböző litológiákra (*Z*=koordinációs szám, *PEX*=perkolációs hatvány kitevő, α=a tekervényes folyadékpálya fraktál-dimenziója)

Рис.10. Оптимальные перколяционные параметры для разного литологического состава (*Z*= координационное число, *PEX*=перколяционная степень, α=фрактал-измерение траектории жидкости

The grain-size of 'siltstone' can be anywhere between 0.0625–0.0039 mm which implies a scatter of more than two orders of magnitude in k_{comp}. Also, the fine sandstones with k <100 md very likely spread over 2 or 3 Wentworth classes (judged from the range of their permeabilities) which explains the large scatter for this lithology.

The scatter of fine-grained samples is further increased by the less reliable measurement of very low permeabilities.

In spite of the known difficulties [MIAN, HILCHIE 1982] of the measurement of *CEC*, GRAVESTOCK, ALEXANDER [1988] found very good correlation between *CEC* values and semiquantitative X-ray diffraction analysis of the < 2 μm size fraction. They were, however 'cautious of accepting semiquantitative XRD data on the standard against which to calibrate wireline logs' [GRAVESTOCk, ALEXANDER 1988, p. 75] and, obviously, the same criticism applies to the calibration involved by Eq. (13) of the present paper.

I am convinced that unless one can estimate the grain-size distribution and sedimentary fabric from digital image analysis of thin sections [BERRYMAN, BLAIR 1986] it is hopeless to aim at a better than order of magnitude agreement between experimental and computed permeabilities over a large porosity and grainsize range. The same conclusion has been

drawn by BERRYMAN and BLAIR [1986] when reviewing recent theories of permeability.

Obviously, the double logarithmic plot of Fig. 9 does not contain those data for which either one or both of k_{meas} and k_{comp} are zero. There were only five such cases: for a 'shaly fine sandstone' sample I had k_{meas}=0 and k_{comp}=0; there were 3 'siltstone' samples and a 'shaly fine sandstone' sample with $0 < k_{meas} < 0.004$ md and k_{comp}=0.

It is possible to deduce the experimentally known interdependences between pressure, permeability and shaliness from a mathematical analysis of Eqs. (26a-f). For increasing pressure porosity will exponentially decrease [HEDBERG 1926], this leads to a decrease in hydraulic radius (Eq. 26c) and in the value of p (Eq. 26e). As some of the throats will close up under pressure, the average coordination number Z will also decrease, that is the percolation threshold p_c becomes larger (Eq. 26f). Consequently, both factors R_{HYD} and $(p - p_c)$ in Eq. (26a) are decreasing with increasing pressure which leads to an overall permeability decrease with increasing pressure.

Compaction has a similar effect: besides the reduction of porosity, the number of long, concavo-convex and sutured contacts between quartz grains would generally increase with depth and age [TAYLOR 1950, SMALLEY 1967], this reduces the average number of bonds belonging to a node in the corresponding percolation lattice (Fig. 8b). The coordination number Z decreases, that is the percolation threshold p_c increases (Eq. 26f). The percolation model also predicts — at least for kaolinite bearing sandstones — that the permeability reduction with increasing compaction is much more serious than porosity reduction.

An increase in kaolinite content λ slightly reduces the hydraulic radius (according to Eqs. 26c,e) but its permeability reducing effect is mainly due to the increased tortuosity described by the percolation function $\tau^2 \sim (p - p_c)^{-PEX}$.

Figure 10, showing the optimum percolation parameters (Z_{opt}, PEX_{opt}) for the different lithologies, deserves a closer lock. Observe that there are two horizontal scales: the percolation exponent PEX and the fractal dimension of the percolating fluid path α. The two values are related by: $PEX = 1.66\,(\alpha - 1)$ for 3-dimensional percolation [RITZENBERGER, COHEN 1984].

For 'clean fine sands' (lithology 3, $k \geq 100$ md) PEX=0, that is there is no percolation transition and tortuosity is constant independently of kaolinite content. 'Siltstones' (lith. 5) and 'shaly fine sand' (lith. 4, $k < 100$ md) have a more complicated pore network (Z=5-6) than 'coarse sands' and 'medium sands' (liths. 1 and 2) where Z=2-4.

The optimal percolation exponent is PEX=0 (no percolation) for 'clean fine sands'; PEX=1.5-2.5 for 'coarse sands' and 'siltstone', PEX=3-5.5 for 'medium sand' and PEX=4.5-5.5 for 'shaly fine sand'. This seems to settle the controversy [THOMPSON et al. 1987] which is the 'correct' percolation

exponent: 1.9 found by KATZ, THOMPSON [1986] or the 'Swiss cheese' model percolation exponent 4.4 of Halperin's group [HALPERIN et al. 1985]. In the present example, 'siltstones' and 'coarse sand' are closer to the KATZ and THOMPSON [1986] model, while 'medium sand' and the low permeability 'shaly fine sand' to the 'Swiss cheese' model [ELAM et al. 1984, HALPERIN et al. 1985]. In general, different percolation exponents can be expected for sands of different grain-size and different clay morphology.

The percolation exponent has a simple physical meaning [RITZENBERGER and COHEN 1984]: by Eq. (23) *PEX* is connected to the fractal dimension of the fluid paths near the percolation threshold.

For the high permeability 'clean fine sand', where there is no percolation transition, the fluid path is one-dimensional. For 'coarse sand' and 'siltstones' $\alpha \approx 2$ which is the fractal dimension of Brownian motion in the 3-dimensional Euclidian space (Table II). This corresponds to the model of MOSOLOV, DINARYEV [1987] who assumed the transfer of fluid particles in a porous rock as a random Brownian motion. For 'medium sands' $\alpha = 1.8-4.3$, for 'shaly fine sand' ($k < 100$ md) $\alpha = 3.7-4.3$.

According to the Alexander-Orbach conjecture [STANLEY 1986] the fractal dimension of a random walk over a d_f-dimensional fractal structure is:

$$d_W = \frac{3}{2} d_f \tag{29}$$

Thus, the tortous fluid paths in 'medium sands' and low permeability 'shaly fine sands' can be visualized as random walks over 1.9–2.9-dimensional and 2.5–2.9-dimensional fractal pore-spaces, respectively. The high fractal dimensionality of the pore space of these sandstones is in conformity with published results of small angle neutron scattering experiments [WONG 1988] where for certain sandstones fractal dimensions as high as 2.96 have been reported.

Equations (26a-f) only apply for sandstones containing 'discrete particle' type clay [NEASHAM 1977], for example, kaolinite. The empirical equation (13) has been established for the Eromanga Basin samples, for any other region similar calibration should be sought between kaolinite content and *CEC*, or between kaolinite content and wireline logs.

The most important finding of the present paper is that the vanishing permeability at and below the percolation threshold can be ascribed to the divergence of tortuosity. I expect this conclusion to remain valid for other clay morphologies, though different percolation models would describe the effect of pore lining (chlorite) and pore bridging (illite) clays. Mixed clay morphologies (as e.g. the Permian sandstones from the Cooper Basin, South Australia, where the illite/kaolinite ratio has been found [SCHULZ-ROJAHN, PHILLIPS 1989] to depend on the grainsize of the host rock) pose an intriguing, if not intractable, challenge.

Acknowledgements

Thanks are due to Dr. D. Gravestock and Ms. E. Alexander of the South Australian Department of Mines and Energy for providing me with a copy of their report [GRAVESTOCK, ALEXANDER 1988] and for their kind permission to use their petrophysical data. They reviewed the first draft of this paper, suggested many useful changes and kindly permitted to reproduce four illustrations of their report [GRAVESTOCK, ALEXANDER 1988] as Figs. (3, 4, 5 and 7) of the present paper.

Also, I greatly appreciate the help and encouragement of Dr. J. Jones of the Department of Geology and Geophysics, University of Adelaide.

REFERENCES

AMAEFULE J. O., KERSEY D. G., MARSCHALL D. M., POWELL J. D., VALENCIA L. E., KEELAND D. K. 1988: Reservoir description: A practical synergistic engineering and geological approach based on analysis of core data. SPE Paper 18167

BERRYMAN J. G., BLAIR S. C. 1986: Use of digital image analysis to estimate fluid permeability of porous materials: Application of two-point correlation functions. J. Appl. Phys. **60**, 6, pp. 1930-1938

BROADBENT S. R. 1954: Discussion on Symposium on Monte Carlo Methods. J. Roy. Statistic. Soc. B. 68 p.

DENSON K. H., SHINDALA A. S., FENN C. D. 1968: Permeability of sand with dispersed clay particles. Water Resource Res. **4**, 6, pp. 1275-1276

DULLIEN F. A. L. 1979: Porous Media. Fluid Transport and Pore Structure. Academic Press, New York

EDMUNDSON H., RAYMER L. L. 1979: Radioactive logging parameters for common minerals. SPWLA 20th Ann. Log. Symp. Trans. Paper O

EFROS A. L. 1986: Physics and Geometry of Disorder. Percolation theory. Mir Publishers, Moscow

ELAM W. T., KERSTEIN A. R., REHR J. J. 1984: Critical properties of the void percolation problem for spheres. Phys. Rev. Letts. **52**, 17, pp. 1516-1519

EREMENKO N. A. 1968: Geology of Oil and Gas. (In Russian) Nedra, Moscow

ESSAM J. W. 1972: Percolation and cluster size. *In*: Domb C. and Green M. S. (Eds.) Phase Transitions and Critical Phenomena. Vol. 2 Academic Press, London-New York pp. 197-270

FISCH R., HARRIS A. B. 1978: Critical behaviour of random resistor networks near the percolation threshold. Phys. Rev. B. **18**, 1, pp. 416-420

GOODE P., SEN P. N. 1988: Charge density and permeability in clay-bearing sandstones. Geophysics **53**, 12, p. 1610-1612

GRAVESTOCK D. I., ALEXANDER E. M. 1986: Porosity and permeability of reservoirs and caprocks in the Eromanga Basin, South Australia. The Australian Petroleum Exploration Association Journal **26**, pp. 202-213

GRAVESTOCK D. I., ALEXANDER E. M. 1988: Eromanga Basin, South Australia, Core and Well Log Study. National Energy Research, Development and Demonstration Programme, Project Number 820, Rept. No. NERDDP/EG89/803

GRAVESTOCK D. I., ALEXANDER E. M. 1989: Petrophysics of oil reservoirs in the Eromanga Basin, South Australia. Proc. of the Cooper and Eromanga Basins Conf. Adelaide, pp. 142-151

GRIM R. E. 1968: Clay Mineralogy (2nd Ed.) McGraw-Hill Book Co., New York

HALPERIN B. I., FENG S., SEN, P. N. 1985: Differences between lattice and continuum percolation exponents. Phys. Rev. Lett. **54**, 22, pp. 2391-2394

HAMILTON E. L. 1972: Compressional wave attenuation in marine sediments. Geophysics **37**, 4, pp. 620-646

HAMMERSLEY J. M. 1983: Origins of percolation theory. *In*: Deutscher G., Zallen R. and Adler J. (Eds.) Percolation Structures and Processes. Ann. Israel Phys. Soc. **5**, pp. 48-57

HEDBERG H. D. 1926: The effect of gravitational compaction on the structure of sedimentary rocks. Bull. AAPG **10**, 11, pp. 1035-1072

KATZ A. J., THOMPSON A. H. 1986: Quantitative prediction of permeability in porous rock. Phys. Rev. B. **34**, pp. 8179-9181

KORVIN G. 1992: Fractal Models in the Earth Sciences. Elsevier, Amsterdam - New York

KUKAL G. C., HILL R. E. 1986: Log analysis of clay volume: an evaluation of techniques and assumptions used in an Upper Cretaceous sand-shale sequence. SPWLA 27th Ann. Log. Symp., Trans., Paper RR

LE GUILLOU J. C., ZINN-JUSTIN J. 1977: Critical exponents for the n-vector model in three dimensions from field theory. Phys. Rev. Lett. **39**, pp. 95-98.

LUBENSKY T. C. 1977: Scaling theory of phase transitions in diluted systems near the percolation threshold. Phys. Rev. B. **15**, 1, pp. 311-314

MANDELBROT B. B. 1982: The Fractal Geometry of Nature. W. H. Freeman and Co., New York

MARTIN K. R., HAMILTON N. J. 1981: Diagenesis and reservoir quality, Toolache Formation, Cooper Basin. The Australian Petroleum Exploration Association Journal **21**, Pt. 1, pp. 143-154

MIAN M. A., HILCHIE D. W. 1982: Comparison of results from three cation exchange capacity (CEC) analysis techniques. The Log Analyst **23**, 5, pp. 10-16

MICHAELS A. S., LIN C. S. 1954: Permeability of kaolinite. Ind. and Eng. Chem. **46**, 6, pp. 1239-1246

MOSOLOV A. B., DINARYEV O. Yu. 1987: Fractal models of porous media. (In Russian) J. Techn. Phys. **57**, 9, pp. 1679-1685

NEASHAM J. W. 1977: The morphology of dispersed clay in sandstone reservoirs and its effects on sandstone shaliness, pore space and fluid flow properties. SPE Paper 6858

PATCHETT J. G. 1975: An investigation of shale conductivity. SPWLA 16th Ann. Log. Symp. Trans., Paper U

PETTIJOHN F. J., POTTER P. E., SIEVER R. 1972: Sand and Sandstone. Springer, Berlin-Heidelberg-New York

RITZENBERGER A. L., COHEN R. J. 1984: First passage percolation: Scaling and critical exponents. Phys. Rev. B. **30**, 7, pp. 4038-4040

SCHULZ-ROJAHN J. P., PHILLIPS S. E. 1989: Diagenetic alteration of Permian reservoir sandstones in the Nappameri Trough and adjacent areas, southern Cooper Basin. Proc. of the Cooper and Eromanga Basins Conf., Adelaide, pp. 629-645

SEN P. N., GOODE P. A., SIBBIT A. 1988: Electrical conduction in clay bearing sandstones at low and high salinities. J. Appl. Phys. **63**, 10, pp. 4832-4840

SERRA O. 1984: Fundamentals of Well-Log Interpretation. I. The Acquisition of Logging Data. Elsevier, Amsterdam-Oxford-New York-Tokyo

SMALLEY I. J. 1967: A simple model of a diagenetic system. Sedimentology, **8**, pp. 27-33

STANLEY H. E. 1986: Form: an introduction to self-similarity and fractal behaviour. *In:* Stanley H. E. and Ostrowsky N. (Eds.) On Growth and Form. Fractal and Non-Fractal Patterns in Physics. Martinas Nijhoff, Publ., Dordrecht, pp. 21-53

STEWARD H. E., BURCK L. J. S. 1986: Improved cation exchange capacity/Q_V determination using the multi-temperature membrane potential test. The Log Analyst **27**, 1, pp. 25-38

TAYLOR J. M. 1950: Pore space reduction of sandstone. Bull. AAPG **34**, 4, pp. 701-716

THOMPSON A. H., KATZ A. J., KROHN C. E. 1987: The microgeometry and transport properties of sedimentary rock. Adv. Phys. **36**, 5, pp. 625-694

VAN OLPHEN H., FRIPIAT J. J. 1979: Data Handbook for Clay Materials and Other Non Metallic Minerals. Pergamon Press, New York

VOLAROVICH M. P., MARMORSHTEIN L. M., MEKLER, Yu. B. 1968: Variation in the structure of the pore space in sandtsones under pressure. (In Russian) Izv. Akad. Nauk. SSSR, Earth Phys. No. **6**, pp. 15-19

VYSSOTSKY V. A., GORDON S. B., FRISCH, H. L., HAMMERSLEY J. M. 1961: Critical percolation probabilities (bond problem). Phys. Rev. **123**, 5, pp. 1566-1567

WALSH J. B., BRACE W. F. 1984: The effect of pressure on porosity and the transport properties of rock. Journal Geophys. Res. **89**, B11, pp. 9425-9431

WARDLAW N. C., MCKELLAR M. 1981: Mercury porosimetry and the interpretation of pore geometry in sedimentary and artificial models. Powder Techn. **29**, pp. 127-143

WONG P.-Z. 1988: The statistical physics of sedimentary rock. Phys. Today **41**, 12, pp. 24-32

ZALLEN R. 1983: Introduction to percolation: A model for all seasons. *In*: Deutscher G., Zallen R. and Adler J. (Eds.) Percolation Structures and Processes. Ann. Israel Phys. Soc. **5**, pp. 4-16

ZIMAN J. M. 1979: Models of Disorder. Cambridge U. Press, Cambridge

KAOLINIT TARTALMÚ HOMOKKŐVEK PERMEABILITÁSÁNAK PERKOLÁCIÓS MODELLJE

KORVIN Gábor

A porózus kőzetek permeabilitására vonatkozó korszerű elképzelések, és a Perkolációs Elmélet alapjainak rövid ismertetése után új modellt vezetek le a diszkrét agyagrészecskéket (kaolinit) tartalmazó agyagos homokkövek permeabilitására. A kísérletileg tapasztalt permeabilitás-csökkenés elegendően nagy agyagtartalom és alacsony, de nem zéró porozitás esetében perkolációs jelenség, annak következtében, hogy a kaolinit részecskék a pórusok közötti áteresztő nyílások ("torkok") kritikus hányadát eltorlaszolják.

A fő eredmény (26a-f egyenletek) a permeabilitás kifejezése a szemcseméret, porozitás és a kaolinit térfogathányad segítségével. Szerepel a képeletben a $(p_c - p)^{PEX}$ perkolációs faktor, amely a tortuozitás divergenciájaként értelmezhető a perkolációs küszöb közelében. A *PEX* perkolációs hatványkitevő egyszerű kapcsolatban áll a tekervényes folyadékpálya fraktál-dimenziójával.

A modellt 229 db, júra - korai kréta korú, az Eromanga medence (Dél-Ausztrália) folyami és tavi eredetű tárolóiból származó, kaolinittartalmú homokkő minta permeabilitásának kiszámítására alkalmaztam. A közelítő diszkrét perkolációs rács koordinációsszámát és a perkolációs hatványkitevőt számítógépes optimumkereséssel határoztam meg, ezenkívül nem volt más illesztési paraméter.

Jó egyezést kaptam a mért és számított permeabilitások között, több mint hét nagyságrenden át. Különböző perkolációs hatványkitevők feleltek meg az egyes litológiáknak: 0 a nagy permeabilitású tiszta homokkőnek, 1,5-2 a durvaszemcsés homokkőnek és a homoklisztnek, 3-5,5 a közepes szemcseméretű homokkőnek és 4,5-5,5 az alacsony permeabilitású (k < 100 md) finomszemcsés homokkőnek.

ПЕРКОЛЯЦИОННАЯ МОДЕЛЬ ПРОНИЦАЕМОСТИ КАОЛИНИТ-СОДЕРЖАЩИХ ПЕСЧАНИКОВ

Габор КОРВИН

После описания современных представлений о проницаемости пористых пород и основ перколяционной теории дается новая модель проницаемости глинистых песчаников, содержащих дискретные глинистые зерна (каолинита). Установленное опытным путем уменьшение проницаемости при достаточно высоком содержании глины и низкой, но отличающейся от нуля, пористости является перколяционным явлением в связи с тем, что зерна каолинита закрывают критическую часть межпоровых отверстий (горловин).

Главным результатом работы являются уравнения 26a-f, выражающие зависимость проницаемости от размера зерен, пористости и объемного содержания каолинита. В формуле имеется перколяционный фактор $(p_c - p)^{PEX}$, который можно понимать как дивергенцию тортуосности вблизи

перколяционного порога. Перколяционная степень PEX имеет простую связь с фрактал-дименсией траектории жидкости.

Модель была применена для вычисления проницаемости 229 образцов каолинит-содержащих песчаников юрского и мелового возраста отобранных из резервуаров речного и озерного происхождения бассейна Эроменджж (Южная Австралия). Перколяционная степень и координационное число приближенной дискретной перколяционной решетки были определены компьютерным способом оптимизации (других параметров сопряжения не было).

Между измеренными и расчетными значениями проницаемости наблюдается хорошее совпадение при диапазоне 7 порядков величины. Перколяционная степень зависит от литологического состава образца : 0–для чистых песчаников высокой проницаемости, 1.5-2–для грубозернистых песчаников и песчаного ила, 3-5.5–для среднезернистых песчаников и 4.5-5.5–для мелкозернистых песчаников низкой проницаемости.